ACS Catalysis

Research Article

pubs.acs.org/acscatalysis

Effects of Helix Macrodipole and Local Interactions on Catalysis of Acyl Transfer by α-Helical Peptides

Q. Nhu N. Nguyen,[†] Michael W. Lodewyk,[§] Silvia Bezer,[‡] Michel R. Gagné,[‡] Marcey L. Waters,[‡] and Dean J. Tantillo*[,†]

[†]Department of Chemistry, University of California—Davis, Davis, California 95616, United States

[‡]Department of Chemistry, University of North Carolina at Chapel Hill, Chapel Hill, North Carolina 27599-3290, United States

[§]Physical Science Department, Butte College, Oroville, California 95965, United States

Supporting Information

ABSTRACT: The impact of the macrodipole of peptide helices on catalysis was examined using density functional theory calculations. Transition state structures for histidine-containing polyalanine nucleophilic catalysts adding to carbonyls were computed, and the impact of both global and local noncovalent interactions was assessed. Although the peptide macrodipole appears to influence energy barriers, local interactions dominate.

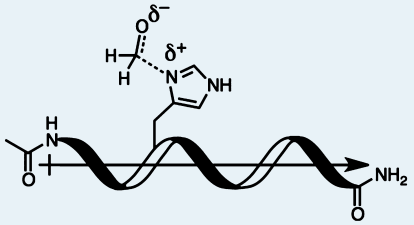

KEYWORDS: *peptide, catalysis, imidazole, π-hole, dipole, α-helix*

INTRODUCTION

It is well-known that α-helical polypeptides have "macrodipoles" oriented along the helical axis (aside from local dipole moment contributions from side-chain residues) as a result of the fact that their backbone carbonyl groups all point toward the C-terminus.[1] These helical dipoles affect, for example, the packing of helices into bundles,[2] interactions with lipid bilayers,[3] and the distribution of charge at binding/active sites.[4] In addition, placement of particular side chains nearer to the C- or N-terminus of helical peptides can affect their structures and reactivity. For instance, Hudgins and Jarrold reported placement of a positively charged lysine residue at the C-terminus of a polypeptide (polyalanines up to 20 residues were examined) facilitates helix formation, whereas placement of the lysine at the N-terminus leads only to globular structures.[5] Carlson and co-workers found that similar helical stabilization could be achieved by adding a negatively charged residue to the N-terminus.[6] In addition, Ren and co-workers showed that the position of a cysteine residue along a peptide chain can also affect its gas phase proton affinity.[7] Although the role of helix macrodipoles in these systems is unclear, the potential for affecting catalytic activity through interactions of reactive groups with macrodipoles sparked our interest. Herein, we examine whether helix macrodipoles can influence the catalytic proficiency of nucleophilic α-helical polypeptide catalysts.

Previously, we described a reactive tagging strategy that uncovered helical polypeptides with histidine residues that function as acyl transfer catalysts in trifluoroethanol (TFE).[8] Application of this strategy led to the observation that a nine-residue polyalanine helix with a histidine as its seventh residue (Figure 1) reacts more quickly (2.4×10^{-7} M s^{-1}) than a nine-residue polyalanine helix with a histidine as its third residue (0.7×10^{-7} M s^{-1}) in trifluoroethanolysis of 4-nitrophenyl 2-methoxyacetate (**A**). We assess herein the origins of this rate difference using density functional theory calculations. Our results indicate that, although macrodipoles are present, they do not control reactivity in these systems. Instead, local interactions dominate.

COMPUTATIONAL METHODS[9]

Optimization and frequency calculations for minima and transition state structures (TSSs) were carried out using the M06-2X/6-31G(d) method as implemented in Gaussian09.[10] Intrinsic reaction coordinate (IRC) calculations[11] were performed for selected TSSs to confirm the identities of the minima to which they are connected. All calculations were carried out in TFE as modeled with the SMD continuum solvation approach.[12] Single point calculations were also carried out for selected TSSs with M06-2X/6-311+G(2d,p) and ωB97XD/6-311+G(2d,p)[13] to assess whether our results are dependent on the basis set size or functional; our results indicate that the order of transition state energies for the best conformations of the 7-His catalyst is not dependent on the nature of the functional or basis set used (see the Supporting Information for details). For electrostatic potential surfaces, isovalues were set at 0.01 (closest to the molecule; this is the value used in Figure 8), 0.0004, and 0.00001, and the potential ranges were −0.17 to 0.17. Initial guesses at the conformation

Received: December 2, 2014
Revised: January 23, 2015
Published: January 28, 2015

DOI: 10.1021/cs5019277
ACS Catal. 2015, 5, 1617−1622

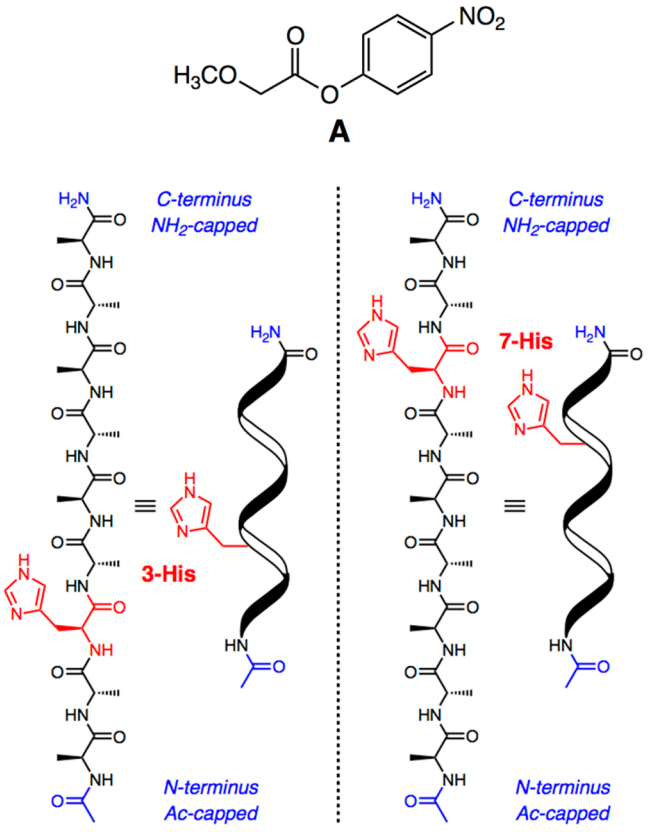

Figure 1. Histidine-containing polyalanine (nine residues total) catalysts examined.

of α-helical backbones were based on α-helices in crystal structures of proteins.

RESULTS AND DISCUSSION

The helix macrodipole is readily visualized via electrostatic potential surfaces. Figure 2 shows such surfaces computed (SMD(TFE)-M06-2X/6-31G(d)) for a nona-alanine α-helix (end-capped as shown in Figure 1). Blue corresponds to the most positive regions, and red corresponds to the most negative regions; the color-mapped potential range is the same for all surfaces. The three surfaces arrayed horizontally differ in terms of the contour of electron density onto which electrostatic potential is mapped. First, these surfaces show clearly that the C-terminus is negatively charged and the N-terminus is positively charged. Upon moving from the surface at the left to that at the right, the difference in charge between the ends of the helix decreases, that is, the effect of the macrodipole falls off with distance from the helical backbone. Figure 2 also shows electrostatic potential surfaces for hexa-, nona-, dodeca-, and pentadeca-alanine helices at a consistent contour of electron density. Although the magnitudes of the electrostatic potential at the termini of these helices remain similar, the charge-neutral (colorless) region at the center of the helix increases in size with an increase in the helix length. Thus, although the net dipole moment of the helix increases as a helix is lengthened (the dipole moment is related not only to the magnitude of positive and negative charges, but also to the distance between them; computed dipole moments for the four helices in Figure 2: 36, 52, 70, and 86 D), the effect of this macrodipole on groups near the middle of the helix is expected to be of minimal importance.

The effect of nucleophile location along the helix was first examined for the two catalysts shown in Figure 1 attacking formaldehyde, a simple, symmetrical carbonyl-based electrophile. Since local charge separation (between the carbonyl oxygen and imidazole ring) is expected to occur during the attack (Figure 3), we wondered whether alignment of the TSS core with the macrodipole might affect the relative energies of the TSSs for the two catalysts, whose histidine attachment points are relatively close to one or the other end of the helix, and their associated barriers for addition.

Although formaldehyde is small and symmetrical, multiple conformations are possible for the TSSs for nucleophilic attack. First, the C_α–CH_2 bond is expected to be a 3-fold rotor (three staggered conformations possible), whereas the CH_2–$C_{imidazole}$ bond is expected to be a 2-fold rotor (Figure 3). Thus, we

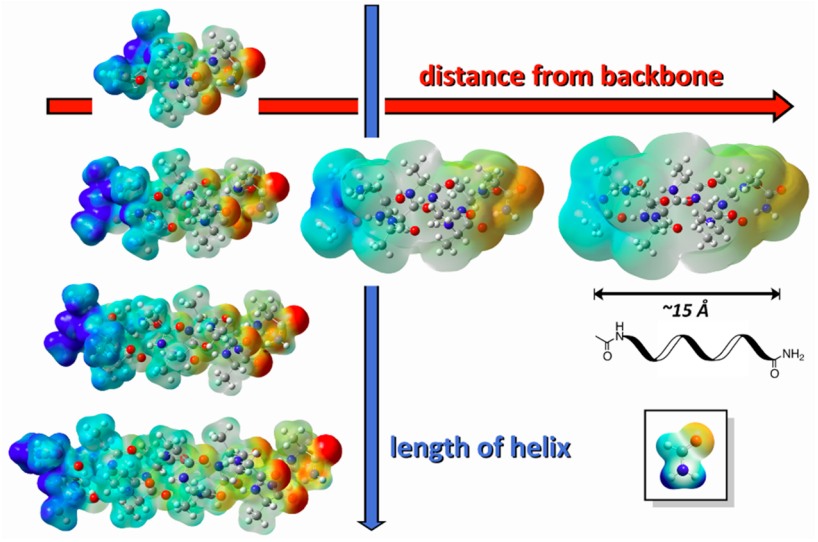

Figure 2. Electrostatic potential surfaces (SMD(TFE)-M06-2X/6-31G(d)); the scale ranges from −0.170 (red) to +0.170 (blue) for a nona-alanine helix at different contours of electron density (horizontal) and electrostatic potential surfaces for hexa-, nona-, dodeca-, and pentadeca-alanine helices at a consistent contour of electron density (vertical). Formamide is shown in the box (bottom right; same scale) for comparison.

DOI: 10.1021/cs5019277
ACS Catal. 2015, 5, 1617−1622

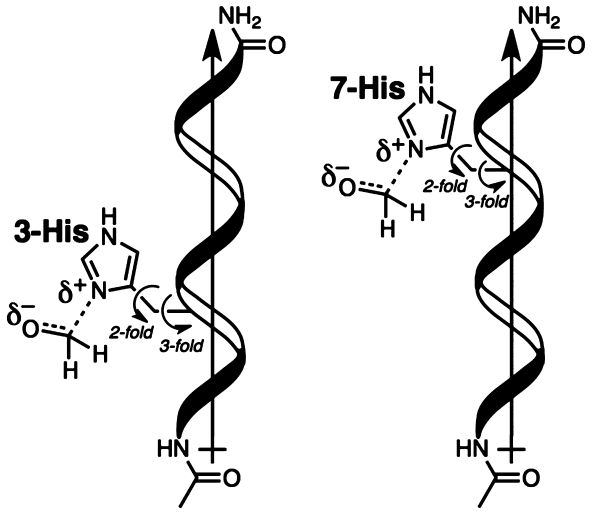

Figure 3. Attack by the polypeptide catalysts from Figure 1 onto formaldehyde. 2-Fold and 3-fold conformational degrees of freedom for the peptide discussed in the text are labeled.

constructed the six resulting conformations for each catalyst and subjected them to full optimizations (alternatives to the α-helix backbone were not examined, given the available experimental data on such systems[8]). In addition, two tautomers for the imidazole ring (differing in the relative positions of the NH proton and $CH_2-C_{imidazole}$ bond) were examined for each. Upon adding to formaldehyde, one introduces another 3-fold rotor ($N\cdots C_{formaldehyde}$ bond), thus tripling the number of structures to be examined for each TSS. We located a total of 38 TSSs (certain combinations of individual bond conformations were found to be geometrically incompatible).

Shown in Figure 4a is the lowest-energy TSS for addition of the 3-His catalyst to formaldehyde, which is associated with a predicted barrier of 11.5 kcal/mol (relative to the lowest-energy 3-His catalyst conformer plus a separate formaldehyde). In this TSS, the formaldehyde oxygen is pointed toward the positive end of the polypeptide. Having the same imidazole conformation, the lowest-energy TSS among those TSSs with the formaldehyde oxygen pointing toward the negative end of the polypeptide is predicted to be 1.9 kcal/mol higher in energy (Figure 4b; another TSS conformation with a different imidazole conformation is at 12.3 kcal/mol; see Figure S1 for details). Note that this reactivity tracks with proximity of the incipient oxyanion from the N-terminus.

A similar scenario was observed for the case of the 7-His catalyst, with the lowest-energy TSS (barrier of 11.0 kcal/mol) having the formaldehyde oxygen oriented toward the positive end of the helix (Figure 5a). The TSS with the same imidazole conformation but the formaldehyde oxygen not pointing toward the positive end of the polypeptide is predicted to be 1.5 kcal/mol higher in energy (Figure 5b; again, another TSS conformation with a different imidazole conformation is at 12.3 kcal/mol; see Figure S2). Higher-energy TSSs for both catalysts also showed small energetic preferences for orientation of the formaldehyde oxygen toward the positive end of the polypeptide for given imidazole conformations. Whether the origins of this effect are global or local is addressed below. Note also that predicted barriers for the 7-His catalyst are slightly lower than those for the 3-His catalyst, consistent with the experimental observation described above, despite the approx-

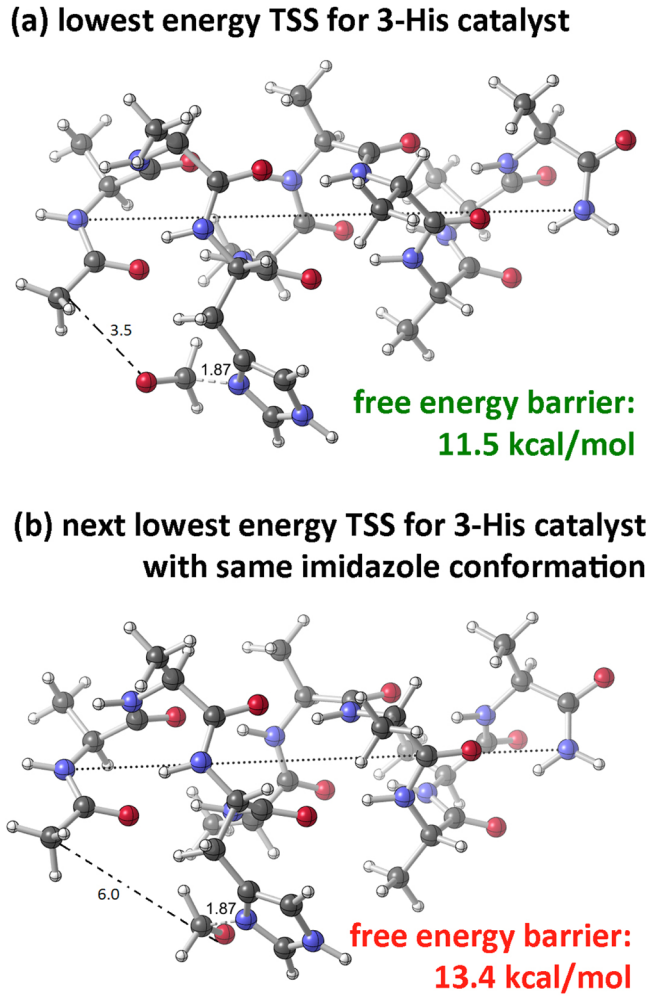

Figure 4. TSSs and predicted free energy barriers (SMD(TFE)-M06-2X/6-31G(d)) discussed in the text for attack on formaldehyde by the 3-His catalyst. Selected distances shown in angstroms. The helical axis is represented by a long dashed line in each structure.

imations (e.g., continuum solvent, model electrophile) in our calculations.

Addition of the 3-His and 7-His catalysts to the ester used experimentally, **A**, was also examined. This ester is less symmetrical than formaldehyde and attack at the two faces of the carbonyl are not equivalent, that is, *re* and *si* attack lead to diastereomeric TSSs, resulting in additional conformational complexity. Figure 6 shows the three lowest-energy TSSs found, all of which happen to be TSSs for the addition of the 7-His peptide. In neither of the two lowest-energy TSSs does the ester carbonyl substructure point along the helical axis. However, in both cases, the nitro group is in close proximity to an end-capping group: in the lower-energy case (Figure 6a), the substrate's nitro group is closer to the C-terminal amide NH_2 group, and in the slightly higher-energy (by 1.2 kcal/mol) case (Figure 6b), the substrate's nitro group is closer to the N-terminal acetyl methyl group. In addition, although the TSS with the nitro group pointing to the N-terminal end cap is slightly lower in electronic energy (and enthalpy), its entropy is slightly worse. Note also that the nitrophenyl group is involved in $C-H\cdots\pi$ interactions[14] in both structures. In the third-lowest energy TSS (Figure 6c), the ester carbonyl points toward the N-terminus of the peptide, with the carbonyl axis roughly

DOI: 10.1021/cs5019277
ACS Catal. 2015, 5, 1617−1622

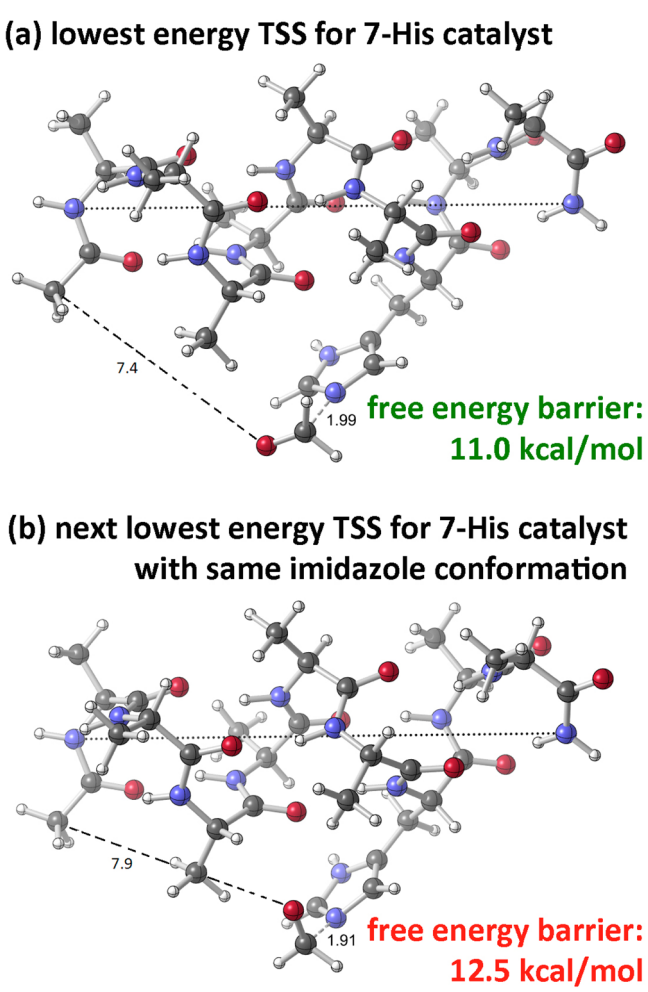

Figure 5. TSSs and predicted free energy barriers (SMD(TFE)-M06-2X/6-31G(d)) discussed in the text for attack on formaldehyde by the 7-His catalyst. Selected distances shown in angstroms. As discussed in the Introduction, the 7-His catalyst is slightly faster than the 3-His catalyst in trifluoroethanolysis of **A**. The helical axis is represented by a long dashed line in each structure.

parallel to the helical axis, but this group is quite far from the helical backbone. It seems clear that the helical macrodipole is not the controlling factor here.

Several small models of the two lowest-energy TSSs shown in Figure 6a,b were also examined to dissect the individual contributions of each interaction (Figure 7).[15] Models including only histidine residues and ester **A** are shown in Figure 7a. Constraining these groups to their positions in the fully optimized TSSs from Figure 6 (truncating the other parts of the peptide and capping with hydrogens at standard X-H distances) leads to a larger separation in their energies, possibly the result of a better oriented C−H···O interaction in the lower-energy TSS (and a C−H···O interaction between an aryl C−H and a backbone carbonyl),[16] recall that the two lowest-energy TSSs differ by only 1.2 kcal/mol in the fully optimized models. Models including **A**, a methyl imidazole model of the nucleophilic histidine side chain and the C- or N-terminal amide group, again constrained to their positions in the fully optimized TSSs from Figure 6 (Figure 7b), display a much smaller gap in TSS energies.[17] A model including **A**, a methyl imidazole model of the nucleophilic histidine side chain, and an internal backbone amide near the nitro group (Figure 7c) is

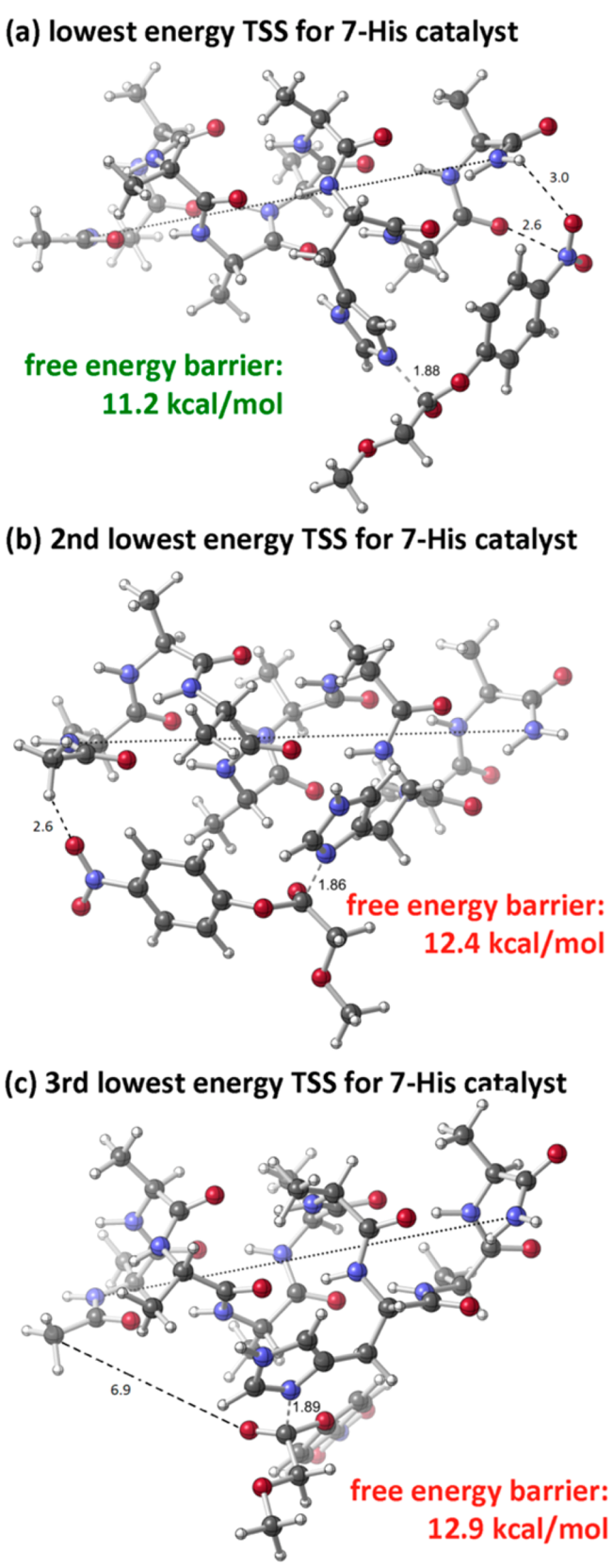

Figure 6. TSSs and predicted free energy barriers (SMD(TFE)-M06-2X/6-31G(d)) discussed in the text for attack on **A** by the 7-His catalyst. Selected distances shown in angstroms. The helical axis is represented by a long dashed line in each structure.

DOI: 10.1021/cs5019277
ACS Catal. 2015, 5, 1617−1622

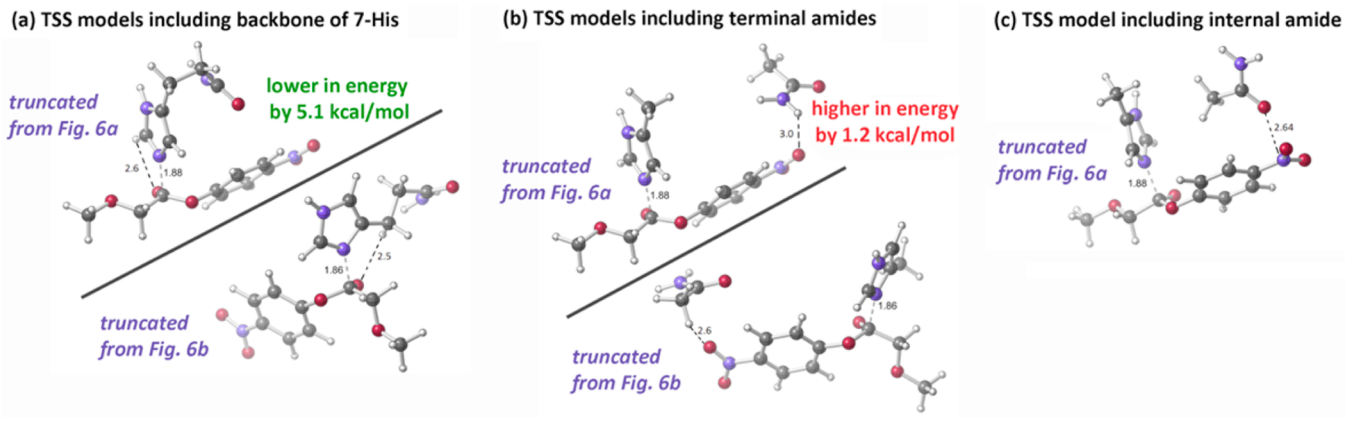

Figure 7. Truncated TSS models and relative energies (SMD(TFE)-M06-2X/6-31G(d); electronic energies) discussed in the text for attack by the 7-His catalyst. Selected distances shown in angstroms.

lower than the best structure in Figure 7b by 3.1 kcal/mol, indicating that the unusual carbonyl lone pair···nitro group interaction (known also as a "π-hole interaction")[18] in this structure is worth more than a C−H···O or N−H···O hydrogen bond to the nitro group. This interaction is largely electrostatic in nature; the N of the nitro group and nearby carbons of the nitrophenyl moiety bear some positive charge, as shown in Figure 8 (top) for the ester used in our experiments, although an interaction with the nitroaryl ester LUMO (Figure 8, bottom) likely also contributes (note also that the O···C_{NO_2} distance in the structure from Figure 6a is 2.9 Å).

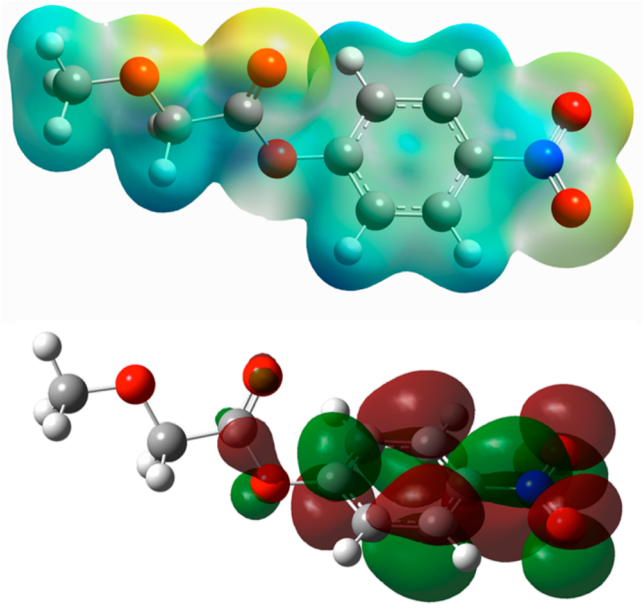

Figure 8. Top: Electrostatic potential surface (SMD(TFE)-M06-2X/6-31G(d)); the scale ranges from −0.170 (red) to +0.170 (blue) for ester **A**. Bottom: LUMO of ester **A**.

The lowest-energy TSSs for addition of the 3-His peptide (Figure 9; ranked fifth and seventh overall) are associated with barriers that are ∼3 kcal/mol larger than the lowest barriers for 7-His attack. These results are qualitatively consistent with the experimental observation that reaction with the 7-His peptide occurs at a faster rate. In the two TSSs shown in Figure 9, the ester carbonyl group is quite far from the peptide backbone.

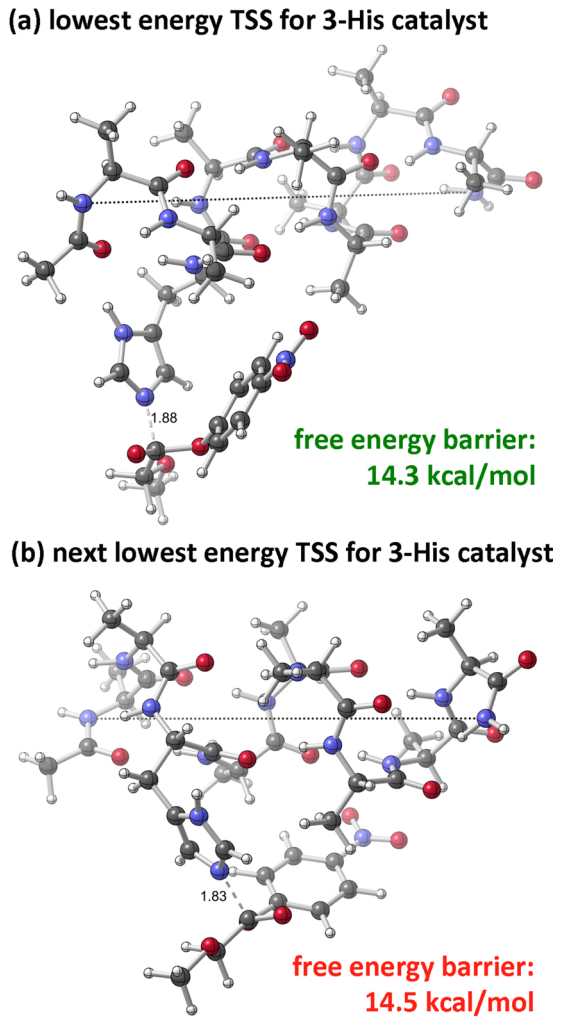

Figure 9. TSSs and predicted free energy barriers (SMD(TFE)-M06-2X/6-31G(d)) discussed in the text for attack on **A** by the 3-His catalyst. Selected distances shown in angstroms. The helical axis is represented by a long dashed line in each structure.

CONCLUSIONS

Our calculations clearly show the presence of a macrodipole along the α-helical structures examined. Although this macrodipole does appear to have an effect on relative energies of TSSs, this effect also appears to be easily overwhelmed by local

DOI: 10.1021/cs5019277
ACS Catal. 2015, 5, 1617−1622

interactions, including those with distal substituents on the substrate leaving group. We continue to look for general principles that will aid in the design of future peptide catalysts. For example, one system described herein makes use of an unusual carbonyl−nitro interaction that may find broader application in catalyst design. The results of our calculations also imply that end-capping a peptide helix with a nucleophile or electrophile could allow the effects of the peptide macrodipole to be expressed in catalytic potency.

■ ASSOCIATED CONTENT

Supporting Information

The following file is available free of charge on the ACS Publications website at DOI: 10.1021/cs5019277

Additional figures mentioned in the text, conformer and transition state energies, single-point energies, small models, coordinates of seleted structures, and the complete Gaussian reference (PDF)

■ AUTHOR INFORMATION

Corresponding Author

*E-mail: djtantillo@ucdavis.edu.

Notes

The authors declare no competing financial interest.

■ ACKNOWLEDGMENTS

We gratefully acknowledge support from the U.S. Defense Threat Reduction Agency (HDTRA1-10-0030) and the National Science Foundation (supercomputing resources through a grant from the XSEDE program: CHE-030089 to D.J.T.).

■ REFERENCES

(1) (a) Pauling, L.; Corey, R. B.; Branson, H. R. *Proc. Natl. Acad. Sci. U.S.A.* **1951**, *37*, 205−211. (b) Hol, W. G. J.; van Duijnen, P. T.; Berendsen, H. J. C. *Nature* **1978**, *273*, 443−446. (c) Hol, W. G. J.; van Duijnen, P. T.; Berendsen, H. J. C. *Nature* **1978**, *273*, 443−446.

(2) (a) Robinson, C. R.; Sligar, S. G. *Protein Sci.* **1993**, *2*, 826−837. (b) Gilson, M. K.; Honig, B. *Proc. Natl. Acad. Sci. U.S.A.* **1989**, *86*, 1524−1528.

(3) (a) Richardson, J. S. *Adv. Protein Chem.* **1981**, *34*, 167−339. (b) Biggin, P. C.; Sansom, M. S. P. *Biophys. Chem.* **1999**, *76*, 161−183.

(4) (a) Spencer, R. H.; Rees, D. C. *Annu. Rev. Biophys. Struct.* **2002**, *31*, 207−233. (b) Hol, W. G. J. *Prog. Biophys. Mol. Biol.* **1985**, *45*, 149−195. (c) Warwicker, J.; Watson, H. C. *J. Mol. Biol.* **1982**, *157*, 671−679. (d) Calabrese, J. C.; Jordon, D. B.; Boodhoo, A.; Sariaslani, S.; Vannelli, T. *Biochemistry* **2004**, *43*, 11403−11416. (e) Davies, C.; Heath, R. J.; White, S. W.; Rock, C. O. *Structure* **2000**, *8*, 185−195. (f) Hol, W. G. J.; van Duijnen, P. T.; Berendsen, H. J. C. *Nature* **1978**, *273*, 443−446.

(5) (a) Hudgins, R. R.; Jarrold, M. F. *J. Am. Chem. Soc.* **1999**, *121*, 3494−3501. (b) Kohtani, M.; Jarrold, M. F. *J. Am. Chem. Soc.* **2004**, *126*, 8454−8458. (c) Kohtani, M.; Jones, T. C.; Schneider, J. E.; Jarrold, M. F. *J. Am. Chem. Soc.* **2004**, *126*, 7420−7421.

(6) Johnson, A. R.; Dilger, J. M.; Glover, M. S.; Clemmer, D. E.; Carlson, E. E. *Chem. Commun.* **2014**, *50*, 8849−8851.

(7) Morishetti, K. K.; Huang, B. D. S.; Yates, J. M.; Ren, J. *J. Am. Soc. Mass. Spectrom.* **2010**, *21*, 603−614.

(8) Bezer, S.; Matsumoto, M.; Lodewyk, M. W.; Lee, S. J.; Tantillo, D. J.; Gagné, M. R.; Waters, M. L. *Org. Biomol. Chem.* **2014**, *12*, 1488−1494.

(9) An excellent recent review on "computational catalysis": Thiel, W. *Angew. Chem., Int. Ed.* **2014**, *53*, 8605−8613.

(10) (a) M06-2X: Zhao, Y.; Truhlar, D. G. *Theor. Chem. Acc.* **2008**, *120*, 215−241. (b) *Gaussian 09, Revision B.01*; Gaussian, Inc.: Wallingford, CT, 2009 (full reference in Supporting Information).

(11) (a) Fukui, K. *Acc. Chem. Res.* **1981**, *14*, 363−368. (b) Gonzalez, C.; Schlegel, H. B. *J. Phys. Chem.* **1990**, *94*, 5523−5527.

(12) Marenich, A. V.; Cramer, C. J.; Truhlar, D. G. *J. Phys. Chem. B* **2009**, *113*, 6378−6396.

(13) Chai, J. D.; Head-Gordon, M. *Phys. Chem. Chem. Phys.* **2008**, *10*, 6615−6620.

(14) Nishio, M. *Phys. Chem. Chem. Phys.* **2011**, *13*, 13873−13900.

(15) (a) Tantillo, D. J.; Chen, J.; Houk, K. N. *Curr. Opin. Chem. Biol.* **1998**, *2*, 743−750. (b) Tantillo, D. J.; Houk, K. N. In *Stimulating Concepts in Chemistry: Theozymes and Catalyst Design*; Wiley-VCH: Weinheim, Germany, 2000; pp 79−88. (c) DeChancie, J.; Clemente, F. R.; Smith, A. J. T.; Gunaydin, H.; Zhao, Y.-L.; Zhang, X.; Houk, K. N. *Protein Sci.* **2007**, *16*, 1851−1866.

(16) Representative examples: (a) Johnston, R. C.; Cheong, P. H.-Y. *Org. Biomol. Chem.* **2013**, *11*, 5057−5064. (b) Yang, H.; Wong, M. W. *J. Am. Chem. Soc.* **2013**, *135*, 5808−5818. (b) Grayson, M. N.; Pellegrinet, S. C.; Goodman, J. M. *J. Am. Chem. Soc.* **2012**, *134*, 2716−2722. (c) Paton, R. S. *Org. Biomol. Chem.* **2014**, *12*, 1717−1720. (d) Maity, P.; Pemberton, R. P.; Tantillo, D. J.; Tambar, U. K. *J. Am. Chem. Soc.* **2013**, *135*, 16380−16383.

(17) Nitro groups as C−H···O hydrogen bond acceptors: Sonoda, Y.; Goto, M.; Tsuzuki, S.; Tanaoki, N. *J. Phys. Chem. A* **2006**, *110*, 13379−13387.

(18) (a) Wozniak, K.; He, H.; Klinowski, J.; Jones, W.l; Grech, E. *J. Phys. Chem.* **1994**, *98*, 13755−13765. (b) Yin, Z.; Jiang, L.; He, J.; Cheng, J.-P. *Chem. Commun.* **2003**, 2326−2327. (c) Paulini, R.; Müller, K.; Diederich, F. *Angew. Chem., Int. Ed.* **2005**, *44*, 1788−1805. (d) Bauzá, A.; Mooibroek, T. J.; Frontera, A. *Chem. Commun.* **2014**, *51*, 1491−1493. Computational results reported in this paper indicate that nitro π-hole interactions, at least in the gas phase, can have binding energies up to ∼7 kcal/mol.

DOI: 10.1021/cs5019277
ACS Catal. 2015, 5, 1617−1622